

Inclusion of Silicon Delta-doped Two-dimensional Electron Gas Layer on Multi-quantum Well Nano-structures of Blue Light Emitting Diodes

Keun joo Kim^a

Department of Mechanical Engineering, Chonbuk National University, Deokjindong 1-ga, Deokjin-gu, Jeonju-si, Jeonbuk 561-756, Korea

^aE-mail : kimk@chonbuk.ac.kr

(Received June 15 2004, Accepted August 6 2004)

The influence of heavily Si impurity doping in the GaN barrier of InGaN/GaN multi-quantum well structures of blue light emitting diodes were investigated by growing samples in metal-organic chemical vapor deposition. The delta-doped sample was compared to the sample with the undoped barrier. The delta-doped sample shows the tunneling behavior and forms the energy level of 0.32 eV for tunneling and the photoemission of the 450-nm band. The photoluminescence shows the blue-shifted broad band of the radiative transition due to the inclusion of Si delta-doped layer indicating that the delta doping effect acts to form the higher energy level than that of quantum well. The dislocation may provide the carrier tunneling channel and plays as a source of acceptor. During the tunneling of hot carrier, there was no light emission.

Keywords : Blue LED, Multi-quantum well, Si delta doping, 2DEG

1. INTRODUCTION

GaN-based semiconductors have been rapid progress in the development of visible light-emitting diodes (LED) and laser diodes[1]. Furthermore, their high chemical stability provides promising application into high-temperature and high power electron devices[2]. The InGaN/GaN multi-quantum well structure (MQW) of LED was adapted for high power active layer for photoemission with the graded well of In composition [3,4]. The In graded MQW structure provides the improved emission efficiency in photoluminescence. Another method to improve the device performance in II-V compound semiconductors is the impurity delta doping.

Si delta-doped GaAs and AlGaAs compound semiconductors have been well studied for the electrical transport properties in high speed and optoelectronic devices[5-7]. The delta-doped layer can be placed at the center of the well, which can achieve high carrier densities in the well but produce limited electron mobilities because the charge carriers and impurities share the same region of space[8]. The delta-doped layer can also be placed outside the well, or in the barrier region, to achieve higher mobilities owing to the fact that the mobile charge carriers are separated from the ionized

impurities[9]. Recently, the growth of Si delta-doped GaN by metal-organic chemical-vapor deposition (MOCVD) has been reported[10-12]. The peak carrier density of Si delta-doping increases with doping time and SiH₄ flow rate, while the full width of half maximum of the carrier profile decreases with both increasing doping time and SiH₄ flow rate. Except for a broadened carrier distribution in GaN induced by Si diffusion due to high growth temperature, the Si delta-doping properties in GaN are similar to those of GaAs.

In this work, we report a study of the introduction of delta doping into InGaN/GaN MQW of blue LED in order to reduce the forward operating voltage. Two samples of 5 periods InGaN/GaN MQW structures were grown by MOCVD with and without the inclusion of heavily Si delta-doped layer in the first barrier. The barrier delta-doped sample provides the tunneling behavior of hot carrier in current-voltage characteristic.

2. EXPERIMENTAL

GaN films were grown by the MOCVD method in the vertical mode of reactor. Sapphire wafer of C (0001) basal plane with a two-inch diameter was used for substrate. Trimethylgallium (TMGa), Trimethylindium

(TMIn), ammonia (NH_3), silane (SiH_4) and bis-cyclopentadienyl magnesium (Cp_2Mg) were used as Ga, In, N, Si and Mg sources, respectively. The substrate was heated to $1055\text{ }^\circ\text{C}$ in a stream of hydrogen and the substrate temperature was then lowered to $520\text{ }^\circ\text{C}$ in order to grow the GaN nucleation buffer layer. The thickness of the buffer layer was about 350 \AA . The $1\text{ }\mu\text{m}$ -thick undoped GaN film and the $2\text{ }\mu\text{m}$ -thick n-type GaN film were sequentially grown at a temperature of $1055\text{ }^\circ\text{C}$ at 500 Torr. The n-type GaN layer was doped with the SiH_4 gas at the flow rate of 638 nano-mol/min. After the growth of the n-type GaN contact layer, the undoped GaN barrier with the inclusion of the Si heavily doped layer was grown. The heavily doped layer has a thickness of 40 \AA , and inside of the middle of the undoped GaN a thickness of 100 \AA , when the flowing SiH_4 gas has a flow rate of 791 nano-mol/min.

The gas flow rates of the quantum active layers in the fabrication process for the heavily doped sample are shown in Fig. 1. The main flow rates of H_2 , NH_3 , and TMGa were kept at 25 slm (liter/min), 30 slm, and $98\text{ }\mu\text{mol}/\text{min}$, respectively, with a growth temperature of $720\text{ }^\circ\text{C}$ at 200 Torr. The 5 periods of InGaN/GaN MQW structure with the thickness of $20/100\text{ \AA}$, and subsequently the Mg doped p-type GaN film with the thickness of $0.12\text{ }\mu\text{m}$, were grown. The growth of the p-type GaN layer was carried out under the following parameters: temperature $1020\text{ }^\circ\text{C}$, pressure 200 Torr, flow rates of TMGa at $293\text{ }\mu\text{mol}/\text{min}$, Cp_2Mg of $15.6\text{ }\mu\text{mol}/\text{min}$, and an NH_3 of 17 slm. The full structure of the LED wafer was processed with the rapidly thermal annealing at $550\text{ }^\circ\text{C}$ in order to achieve Ohmic contacts.

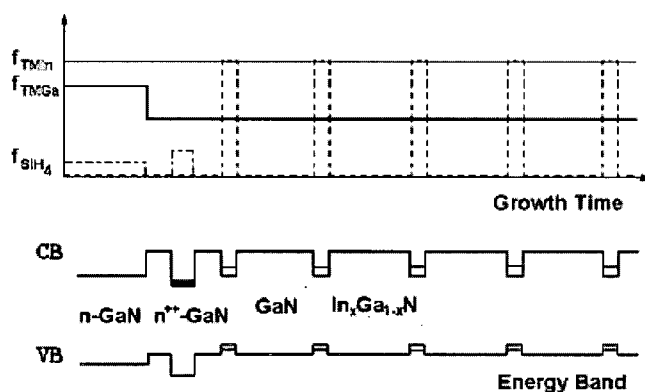


Fig. 1. Schematic diagram of Gas flow rates of InGaN/GaN MQW structure. After growth of n-type GaN Ohmic contact layer, the undoped GaN barrier layer including the Si delta doped layer was introduced by the modulation of the gas flow rates.

Figure 2 shows the full structure of the LED sample including the heavily Si delta-doped GaN layer within the undoped barrier. Before starting the growth of 5 periods InGaN/GaN MQW structures with well widths of 20 \AA and barrier widths of 100 \AA , the undoped GaN barrier including the intermediate Si delta-doped layer was grown at the temperature of $720\text{ }^\circ\text{C}$. Furthermore, the single layer structures such as a Si doped n-type GaN film, a Si delta doped layer in undoped thin GaN layer on n-type GaN film, and a Mg doped p-type GaN film were grown for the structural evaluations of physical properties.

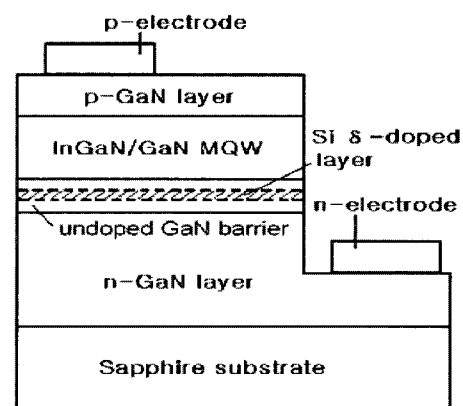


Fig. 2. The blue LED structure of the 5 periods InGaN/GaN MQW with the inclusion of Si delta doped layer.

From Hall effect measurement, the carrier concentrations of n- and p-type contact layers were evaluated to the values of 6.0×10^{18} and $2.2 \times 10^{17}/\text{cm}^3$, which are corresponding to the electron quasi-Fermi level of 34 meV from conduction band edge and to the hole quasi-Fermi level of 0.13 eV from valence band edge, respectively. The undoped GaN layer and the Si delta doped layer show the carrier concentrations of 5.3×10^{17} and $8.6 \times 10^{19}/\text{cm}^3$, respectively. This indicates that the Si delta doping may provide the formation of two-dimensional electron gas layer.

3. RESULTS AND DISCUSSION

In the context of the fabrication of LED device, the Ohmic property of p-GaN and Ni/Au alloy was analyzed in terms of the annealing temperature on the p-type contact layer as shown in Fig. 3. The resistance is not monotonically decreased with increasing annealing temperature. The optimum annealing temperature is about $450\text{ }^\circ\text{C}$. As increasing the temperature, the reaction of p-GaN and Ni/Au alloy enhances the linearity of Ohmic character and surface built-in potential barrier decreases. However, the linearity is still required to

improve indicating the limitation of the reduction of work function. The further increase of the temperature provides the deteriorated quality of current-voltage (I-V) characteristic.

According to Ishikawa et al.[13], Ni/Au provides the lowest resistance for the annealing temperature of 500 °C among their samples of Ta, Au, Pt, Ni metals and Ni/Au alloy. They concluded the improvement of the current inject is due to the removal of the surface contamination layer and the reaction between the GaN and the contact metals.

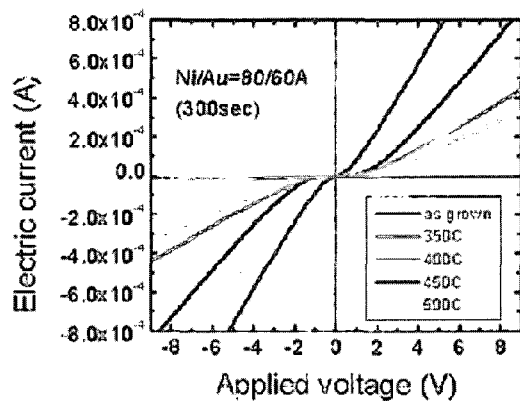


Fig. 3. I-V characteristics on the p-type GaN ohmic contact of Au/Ni alloy with the thickness of 80/60 Å for various annealing temperatures, respectively. The optimal annealing temperature was picked up at 450 °C. However, there still exists a tiny Schottky built-in potential.

The electrical properties on the Mg related defect in the p-type GaN layer were extensively investigated in terms of the p-type transport channel induced by the deep hole trap centers[14,15]. Furthermore, the wide band gap of GaN provides the quasi-Fermi level close to valence band edge with the energy interval of about 0.13 eV at a hole carrier concentration of $2.2 \times 10^{17} / \text{cm}^3$ [16,17]. Therefore, the Ohmic character in p-type contact layer is very difficult to achieve the reduced operating voltage with the limited work functions of various metals. The reactive interface of metal-semiconductor contact by thermal annealing is the alternative method to achieve Ohmic contact. The Mg doping effect and thermal annealing effect on the p-type Ohmic contact property should be microscopically analyzed elsewhere.

Figure 4 shows the PL spectra from MQW structures with the Si delta-doped layer (sample: barr) and without this layer (sample: st). The PL spectrum measured at room temperature for the sample including the heavily doped layer shows a relatively strong emission peaked at 475.1 nm and an FWHM at 211 meV. This is compared

with the peak of 480.1 nm when the FWHM is at 172 meV for the sample without the Si delta-doped layer. The delta doping provides a blue shift of PL emissions and activates on the side of short wavelength implying that the Si delta-doped layer influences on the distortion of the energy states of MQW structure.

The PL spectra from the delta-doped sample show the separated PL bands into 475.1 and 447.2 nm. This band is different from the 2.2 eV-yellow band from n-GaN layer and the Mg defect-related PL band of p-type GaN at 3.0-3.1 eV. Furthermore, the extra band has no relationship to the excitonic level of GaN at 3.4eV. As decreasing the temperature, both samples show the strongly enhanced PL intensity and the undoped sample shows a tiny blue shift at 200 K and a red shift of PL below 100 K. The delta-doped sample shows also same trend to the undoped sample. This should be studied in elsewhere. In this work, we are interested in the analysis to the extra PL band.

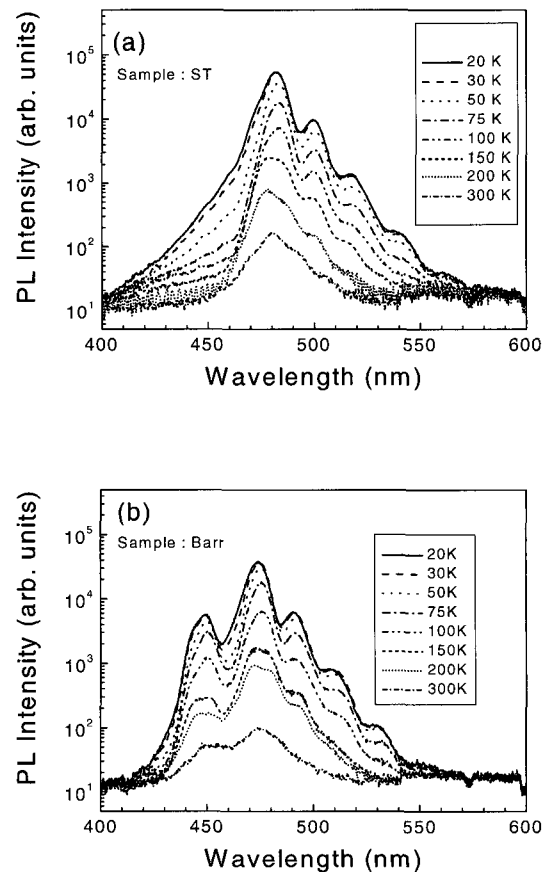


Fig. 4. Temperature-dependent photoluminescence spectra for the samples (a) without and (b) with the inclusion of Si delta doped layer on the same 5 periods InGaN/GaN MQW LEDs.

The extra band can be explained with the schematic diagram of the conduction energy band as shown in Fig. 5. The electron wavefunction is influenced on strong correlation between the delta potential and the QW potential. The energy level of delta potential is a little bit higher than that of the QW, which is consistent with the PL spectra of the delta-doped sample. The delta-doped layer provides another photo-excitation level, which is strongly correlated with the QW PL emission. The impurity level of delta-doped space charge region can also play a trap center of majority carrier. The PL peak energy of 2.57-2.63 eV provides the indium (In) composition range of $x=0.27-0.29$ with the correction of stress effect into empirical bowing factor of 1.00 eV [18,19].

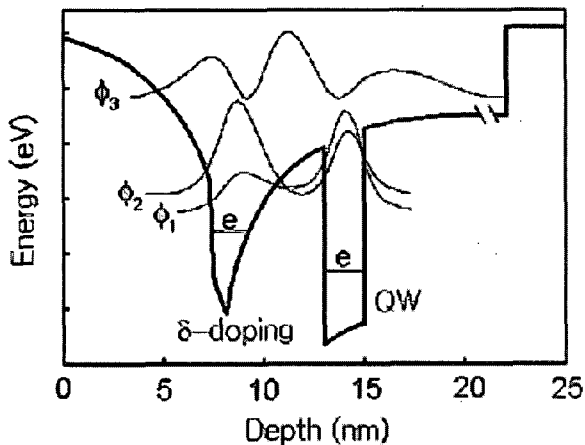


Fig. 5. Schematic energy band diagram of GaN quantum barrier layer with the inclusion of the Si delta doped layer in the vicinity of the first InGaN quantum well layer. The delta-doped layer reduces strain-induced band distortion and forms an energy level.

The I-V characteristics of delta-doped and undoped samples are shown in Fig. 6. The forward voltage of the undoped sample is 5.7 V at 20 mA. The delta-doped sample shows the peak current of 66 mA at 5.2 V and valley current of 20 mA at 5.7 V. Generally, the large static resistance defined as an average resistance in the current interval from 0 to 20 mA is attributed to the internal device structure and the large dynamic resistance as an instantaneous resistance at the current of 20 mA is correlated to Ohmic contact property. At the forward current of 20 mA, the undoped sample shows the static resistance of 285 Ω and the dynamic resistance of 30 Ω . The delta-doped sample shows the abnormal diode character in I-V behavior to compare to the undoped sample. The Si delta doping effect indicates that the tunneling phenomenon of carrier is occurred.

For the forward bias up to 3 V, the component of

tunneling current is dominant with the FWHM of 0.64 eV for the second derivative of I-V characteristics. This indicates that there exists an energy level at 0.32 eV [20]. In the bias region between 3 and 5.7 V, the both components of tunneling and thermal diffusion currents are superimposed. Above the voltage of 5.7 V, the pure thermal diffusion current is the main one.

The energy diagram of a multi-layered structure including Si delta-doped layer can be analyzed shown in Fig. 5. The 2 DEG structure can supply electron into quantum wells through the process of quantum tunneling. The electron wave function in delta potential is strongly correlated with quantum well and the voltage bias enhances electron tunneling. This 2 DEG layer can also spread the electron density to be uniformly recombined with holes in the whole area. The undoped GaN barrier including 2 DEG plays a role of a space charge region where tunneling and injection can be occurred.

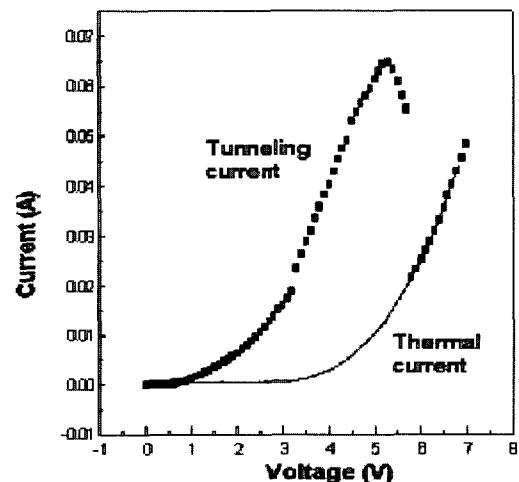


Fig. 6. I-V characteristics of tunneling-type (square dot line:barr) and Schottky-type (solid line:st) for 5 periods InGaN/GaN MQW LED with and without the Si delta-doped layer, respectively.

And also, the injection and the recombination can be occurred in QW active layer. However, the tunneling process is mainly occurred in the space charge region and radiative recombination is in the QW active layer. During the tunneling process, no electroluminescence was observed.

The thermal diffusion current was gradually turned on and the tunneling current was superimposed on the thermal diffusion current in I-V curves. The tunneling barrier height (ϕ_b) of 0.49 eV for the heavily doped quantum barrier can be estimated using the equation of carrier density ($n^{++} = 8.6 \times 10^{19} / \text{cm}^3$),

$$n^{++} = \frac{2K\epsilon_0\phi_b}{qX_b^2}, \quad (1)$$

where $K = 9.8$ is the dielectric constant of the GaN layer, $q = 1.6 \times 10^{-19} \text{ C}$ the electric charge of carrier, ϵ_0 vacuum electric permittivity and X_b equals a tunneling barrier width of 4 nm.

The bright field image of transmission electron microscope (TEM) on InGaN/GaN multi-quantum well nano-structures is shown in Fig. 7. There exist large misfit dislocations originated from the interface between GaN buffer and sapphire wafer. The dislocation can pass through the quantum active region and are partially relaxed in the GaN quantum barrier and the InGaN quantum well, which are shown as a narrow band and a line, respectively. The density of dislocation approximately is the order of $4 \times 10^8 / \text{cm}^2$.

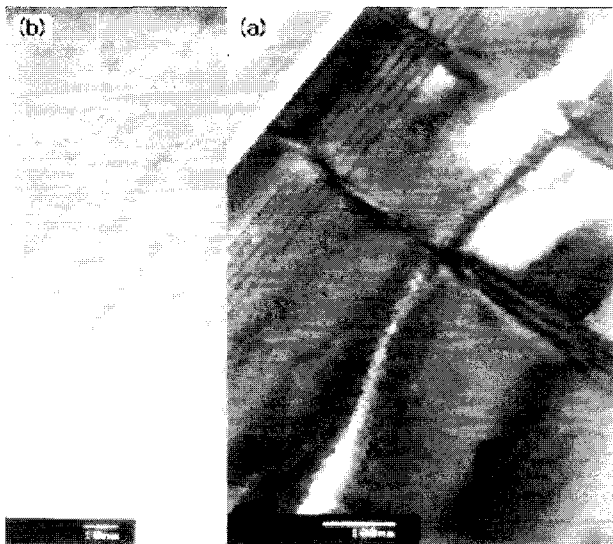


Fig. 7. The micro-structural TEM images in (a) bright field and (b) high resolution modes of InGaN/GaN quantum well nano-structures.

The threading edge dislocation with Burgers vector $a[11\bar{2}0]/3$ forms a relaxed core with the severely distorted bond length and angle in GaN [21]. The core atom on the Burgers circuit forms the threefold coordinated Ga(N) atoms, which can be relaxed towards $sp^2(sp^3)$ leading to empty Ga lone pairs pushed towards the conduction band minimum (CBM), and filled lone pairs on N atoms lying near the valence band maximum (VBM). This threading dislocation is electrically activated with forming the Ga vacancy [22,23]. The vacancy has the acceptor-like nature in n-type GaN.

The InGaN/GaN active layer is shown by high resolution TEM image. The widths of GaN quantum barrier and InGaN quantum well are 10 and 2 nm, respectively. The contrast image near quantum well layer represents dislocation-induced stress field and the Ga vacancy is replaced by the In vacancy. In the context of the acceptor character of dislocation passing through the active layer of quantum wells, the tunneling channel may be formed from the Si delta doped layer to the dislocation pipeline. This tunneling leakage through dislocation provides no radiation and the strong voltage bias supplies carrier into the quantum well region for the radiative recombination.

The chip-on-wafer blue emission of 5 periods MQW InGaN/GaN LEDs under the dc voltage of 7 V was observed as shown in Fig. 8. The inset is the manufactured sample of LED chip. For the LED fabrications, the surface of the p-type GaN layer was partially etched until the n-type contact layer was exposed. The etching process was performed by the implementation of the inductively coupled plasma (ICP) of Cl_2 etching gas.

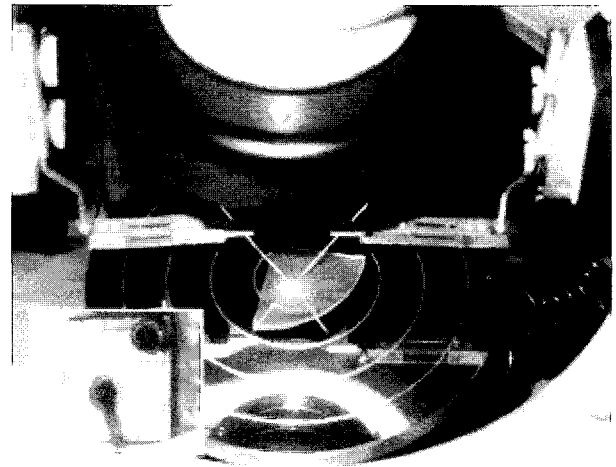


Fig. 8. Blue light emission image of chip-on-wafer of 5 periods MQW InGaN/GaN LEDs under the dc voltage of 7 V. The inset is the manufactured sample of LED chip.

For metal Ohmic contacts, the Ni/Au and Ti/Al metal layers were evaporated onto the p-type GaN with the doping level of $6.5 \times 10^{17} / \text{cm}^3$ [24] and n-type GaN contact layers by utilizing an e-beam evaporator, respectively. For chip separation, the back lapping process of sapphire wafer to a thickness of 0.08 mm can be achieved in home-made lapping system. Finally, by scribing the surface of wafer along the scribing line by diamond tip and by breaking wafer with knife-edge, LED wafers can be separated into square dies with the dimension of $0.35 \times 0.35 \text{ mm}^2$.

4. SUMMARY

In summary, the heavily Si-delta doped barrier was included in the growth of the InGaN/GaN multi-quantum well structures of blue light emitting diodes by using metal-organic chemical vapor deposition. The delta-doped sample was compared to the sample with the undoped barrier. The photoluminescence shows the blue-shifted broad band of the radiative transition due to the inclusion of Si delta-doped layer indicating the higher energy level than that of quantum well. The delta-doped sample shows the tunneling behavior and the energy level of 0.32 eV for tunneling. As increasing the forward bias, the both channels of tunneling and thermal diffusion current are superimposed. The tunneling may be related to the threading edge dislocation because the dislocation line provides the carrier channel as a source of acceptor throughout the quantum active layers. During the tunneling of hot carrier, no light emission was observed.

ACKNOWLEDGMENTS

This work was supported through a Korean Research Foundation Grant (KRF-2002-003-D00126).

REFERENCES

- [1] S. Nakamura and G. Fasol, "The blue laser diode, Springer-Verlag", Berlin, p. 206, 1997.
- [2] T. Egawa, H. Ishikawa, M. Umeno, and T. Jimbo, "Recessed gate AlGaN/GaN modulation-doped field-effect transistors on sapphire", *Appl. Phys. Lett.*, Vol. 76, No. 1, p. 121, 2000.
- [3] T. Onuma, Y. Uchinuma, E. K. Suh, H. J. Lee, T. Sota, and S. F. Chichibu, "Improved emission efficiency in InGaN/GaN quantum wells with compositionally-graded barriers studied by time-resolved photoluminescence spectroscopy", *Jpn. J. Appl. Phys.*, Vol. 42, Pt. 2, No. 11B, p. L1369, 2003.
- [4] G. S. Shin, S. W. Hwang, and K. Kim, "Time-resolved photoluminescence measurement of Frenkel-type excitonic lifetimes in InGaN/GaN multi-quantum well structures", *Trans. EEM*, Vol. 4, No. 5, p. 19, 2003.
- [5] T. R. Block, M. Wojtowicz, A. C. Han, S. R. Olson, A. K. Oki, and D. C. Streit, "Multiwafer molecular beam epitaxy for high volume production of GaAs/AlGaAs heterojunction bipolar transistor wafers", *J. Vac. Sci. Technol. B*, Vol. 16, No. 3, p. 1475, 1998.
- [6] Y. F. Zhang and J. Singh, "Charge control and mobility studies for an AlGaN/GaN high electron mobility transistor", *J. Appl. Phys.*, Vol. 85, No. 1, p. 587, 1999.
- [7] T. Wang, J. Bai, S. Sakai, Y. Ohno, and H. Ohno, "Magneto-transport studies of AlGaN/GaN heterostructures grown on sapphire substrates: Effective mass and scattering time", *Appl. Phys. Lett.*, Vol. 76, No. 19, p. 2737, 2000.
- [8] T. Sekiguchi, Y. Miyamoto, and K. Furuya, "Influence of impurities on the performance of doped-well GaInAs/InP resonant tunneling diodes", *Jpn. J. Appl. Phys.*, Vol. 32, Pt. 2, No. 2B, p. L243, 1993.
- [9] Z. Huang, R. Yu, C. Jiang, T. Lin, Z. Zhang, and J. Chu, "Influence of doping position on subband properties in In_{0.2}Ga_{0.8}As/GaAs heterostructures", *Phys. Rev. B*, Vol. 65, No. 20, p. 205312, 2002.
- [10] E. F. Schubert, "Delta doping of III V compound semiconductors: Fundamentals and device applications", *J. of Vac. Sci. & Technol. A*, Vol. 8, No. 3, p. 2980, 1990.
- [11] J. H. Kim, G. M. Yang, S. C. Choi, J. Y. Choi, H. K. Cho, K. Y. Lim, and H. J. Lee, "Si delta doped GaN grown by low-pressure metalorganic chemical vapor deposition", *MRS Internet J. Nitride Semicond. Res.*, 4S1, G3. p. 49, 1999.
- [12] G. Y. Zhao, M. Adachi, H. Ishikawa, T. Egawa, M. Umeno, and T. Jimbo, "Growth of Si delta-doped GaN by metalorganic chemical-vapor deposition", *Appl. Phys. Lett.*, Vol. 77, No. 14, p. 2195, 2000.
- [13] H. Ishikawa, S. Kobayashi, Y. Koide, S. Yamasaki, S. Nagai, J. Umezaki, M. Koike, and M. Murakami, "Effects of surface treatments and metal work functions on electrical properties at p-GaN/metal interfaces", *J. Appl. Phys.*, Vol. 81, No. 3, p. 1315, 1997.
- [14] A. Y. Polyakov, N. B. Smirnov, A. V. Govorkov, A. S. Usikov, N. M. Shmidt, and W. V. Lundin, "Deep centers spectra and scanning electron microscope studies of p-GaN films prepared by metal-organic chemical vapor deposition on sapphire", *Solid State Electron.*, Vol. 45, No. 2, p. 255, 2001.
- [15] A. Y. Polyakov, A. V. Govorkov, N. B. Smirnov, A. E. Nikolaev, I. P. Nikitina, and V. A. Dmitriev, "Studies of defects in Mg doped p-GaN films grown by hydride vapor phase epitaxy on SiC substrates", *Solid State Electron.*, Vol. 45, No. 2, p. 261, 2001.
- [16] K. Kim and S. J. Chung, "Thermal quenching effect of an infrared deep level in Mg-doped p-type GaN films", *Appl. Phys. Lett.*, Vol. 80, No. 10, p. 1767, 2002.
- [17] H. Nakayama, P. Hacke, M. R. H. Khan, T. Detchprohm, K. Hiramatsu, and N. Sawaki, "Electrical transport properties of p-GaN", *Jpn. J.*

- Appl. Phys., Vol. 35, Pt. 2, No. 3A, p. L282, 1996.
- [18] S. Nakamura, T. Mukai, and M. Senoh, "Si-doped InGaN films grown on GaN films", Jpn. J. Appl. Phys., Vol. 32, Pt. 2, No. 1A/1B, p. L16, 1993.
- [19] K. Osamura, S. Naka, and Y. Murakami, "Preparation and optical properties of Ga_{1-x}In_xN thin films", J. Appl. Phys., Vol. 46, No. 8, p. 3432, 1975.
- [20] M. Tsuchiya and H. Sakaki, "Tunneling spectroscopy of resonant transmission coefficient in double barrier structure", Jpn. J. Appl. Phys., Vol. 30, Pt. 1, No. 6, p. 1164, 1991.
- [21] J. Elsner, R. Jones, P. K. Sitch, V. D. Porezag, M. Elstner, Frauenheim, M. I. Heggie, S. Oberg, and P. R. Briddon, "Theory of threading edge and screw dislocations in GaN", Phys. Rev. Letts., Vol. 79, No. 19, p. 3672, 1997.
- [22] A. F. Wright and U. Grossner, "The effect of doping and growth stoichiometry on the core structure of a threading edge dislocation in GaN", Appl. Phys. Lett., Vol. 73, No. 19, p. 2751, 1998.
- [23] D. C. Look and J. R. Sizelove, "Dislocation scattering in GaN", Phys. Rev. Lett., Vol. 82, No. 6, p. 1237, 1999.
- [24] K. Kim and S. J. Chung, "The Mg solid solution for the p-type activation of GaN thin films grown by metal-organic chemical vapor deposition", Trans. EEM, Vol. 2, No. 4, p. 24, 2001.